Articles

Preparation and Characterization of Magnesium Hydroxide Sulfate Hydrate Whiskers

Yi Ding,[†] Guangtao Zhang,[†] Shuyuan Zhang,[‡] Xinming Huang,[§] Weichao Yu,[†] and Yitai Qian*[,†,‡]

Nanochemistry Laboratory, Department of Chemistry, University of Science and Technology of China, Hefei 230026, People's Republic of China, Structure Research Laboratory, University of Science and Technology of China, Hefei 230026, People's Republic of China, and Department of Material Science and Engineering, Hefei University of Technology, Hefei 230009, People's Republic of China

Received March 21, 2000. Revised Manuscript Received June 9, 2000

Reaction of magnesium sulfate with aqueous ammonia in a hydrothermal condition (150−180 °C) produced a fibrous magnesium hydroxide sulfate hydrate (MHSH) with a composition corresponding to a stoichiometry of $4.34Mg(OH)_2 \cdot MgSO_4 \cdot xH_2O$. Chemical composition analysis showed that the quantity of x was more likely to be 2 rather than the well-known 3. The MHSH whiskers were about 0.3−2 μm in diameter and 40−100 μm in length, with an aspect ratio no less than 100. Selected area electron diffraction (SAED) and X-ray diffraction patterns (XRD) showed the whiskers were well-crystallized with an orthorhombic structure. An interesting superlattice was observed from the ED patterns but this superstructure was unstable under the radiation of a high-energy electron beam especially under HREM conditions. Several techniques such as XRD, TEM, EDS, HREM, XPS, TGA-DTA, FTIR, etc. were used to characterize the structural features and thermal behavior of the experimental products. Our sample of fibrous MHSH was found to lose two hydration waters at about 330 °C, to further decompose at higher treatment temperature, and to transform finally into MgO near 1000 °C.

Introduction

Magnesium hydroxide sulfate hydrates (MHSHs) include a relatively large group of compounds whose interesting properties have been attracting the attention of scientists from various fields, such as chemistry, material science, crystallography, geology, and even mineralogy.[1−11] Geologically called *caminite*, MHSH was first identified in nature in a seafloor hydrothermal system in 1978.[1] As Bischoff and Seyfried originally pointed out, the formation and precipitation of caminite in midocean ridge hydrothermal systems is a potentially important geochemical process with profound effects on subseafloor-alteration processes.[1−3] MHSH can also be called basic magnesium sulfate, or a solid solution in the $Mg(OH)_2-MgSO_4-H_2O$ system. By varying the ratio of these three compounds, the family of MHSHs, $xMg(OH)_2 \cdot yMgSO_4 \cdot zH_2O$ ($x-y-z$ phase) comprises no less than 20 members, either stoichiometric or nonstoichiometric. In the ceramic field, the $MgO-MgSO_4-H_2O$ system has been the subject for numerous investigations in the past few decades because several MHSHs have been shown as promising cements and building materials.[4−6] Recently, some MHSH fibers, especially for the 5−1−3 phase, were proved to be well-suited as an additive for resin, filler, filter medium, or reinforcements of polymers and plastics.[7−9]

Although previous papers have emphasized the potential applications of this material, systematic information on its synthesis and structure characterization of the material are lacking. Often, only some isolated data concerning preparation,[8] structure,[10] and thermal behavior[4−6,11] of MHSHs were reported together with the description of their properties.[7,9] Furthermore, owing to unsystematic investigation of the material, some contradictory results were reported. For example, the crystal structure for the 5−1−3 phase ($5Mg(OH)_2 \cdot$

[†] Nanochemistry Laboratory, Department of Chemistry, University of Science and Technology of China.
[‡] Structure Research Laboratory, University of Science and Technology of China.
[§] Hefei University of Technology.

(1) Bischoff, J. L.; Seyfried, W. E. *Am. J. Sci.* **1978**, *278*, 838.
(2) Janecky, D. R.; Seyfried, W. E., Jr. *Am. J. Sci.* **1983**, *283*, 831.
(3) Haymon, R. M.; Kastner, M. *Am. Miner.* **1986**, *71*, 819.
(4) Kahle, K. *Neue Bergbautech* **1972**, *2* (3), 224.
(5) Kahle, K. *Silikattechnik* **1972**, *23* (5), 148.
(6) Luo, J. G.; Yao, J. S.; Sun, J. E. *J. Chin. Ceram. Soc.* **1998**, *26* (2), 157.
(7) Iwanaga, H.; Yamaguchi, T. *Zairyo Kagaku* **1996**, *33* (4), 155.
(8) Iwanaga, H.; Reizen, K.; Matsunami, T. *Gypsum Lime* **1991**, *235*, 504.
(9) Iwanaga, H.; Iwasaki, T.; Reizen, K.; Matsunami, T.; Ichihara, M.; Takeuchi, S. *J. Am. Ceram. Soc.* **1992**, *75* (5), 1297.
(10) Fleet, M. E.; Knipe, S. W. *Acta Crystallogr.* **1997**, *B53* (3), 358.
(11) Litvinov, S. D.; Lepeshkov, I. N.; Danilov, V. P.; Krasnobaeva, O. N. *Zh. Neorg. Khim.* **1984**, *29* (1), 61.

10.1021/cm000249f CCC: $19.00
Published on Web 09/21/2000

$MgSO_4 \cdot 3H_2O$) was thought to be orthorhombic,[12] tetragonal,[9] and even monoclinic.[4]

In the present article, a systematic investigation has been carried out on the fibrous MHSH(5−1−3) that was prepared by a hydrothermal route using magnesium sulfate and aqueous ammonia as the reactants. X-ray powder diffraction (XRD), transmission electron microscopy (TEM), energy-dispersive X-ray fluorescence (EDAX), high-resolution electron microscopy (HREM), energy dispersive spectrum (EDS), selected area electron diffraction (SAED), X-ray photoelectron spectroscopy (XPS), elemental analysis (EA), thermogravimetric analysis (TGA-DTA), and Fourier transform infrared (FTIR) spectrum were employed to characterize the structural features and thermal behavior of the MHSH samples. Analysis of the results showed that the produced MHSH are well-crystallized whiskers with an aspect ratio no less than 100. Also, an interesting superlattice is observed. Chemical composition analysis shows that the 5−1−3 phase is in fact more likely to be the orthorhombic 5−1−2 phase.

Experimental Section

A. Preparation of MHSH Whiskers. MHSH samples were synthesized by the hydrothermal method.[8,13] All reagents were analytically pure. White powder containing 0.01 mol magnesium sulfate was placed into a Teflon-lined autoclave of 50 mL capacity. Then, the autoclave was filled with aqueous ammonia up to 80% of the total volume. The pH of this mixed solution was around 11. The autoclave was then sealed into a stainless steel tank, and maintained at 150 °C for 16 h without shaking or stirring. After the autoclave was cooled to room temperature naturally, a white gellike precipitate was filtered, and the final mixture had a pH of about 9. The precipitate was washed with distilled water and absolute ethanol for several times, and then dried in a vacuum at 60 °C for 4 h. Finally, a beautiful soft fibrous powder with a white color was obtained. This powder can easily dissolve in hydrochloric acid but shows no obvious dissolvibility in water or basic solution at room temperature. The yield of this method is up to 80−90%.

B. Characterization. X-ray powder diffraction (XRD) patterns were obtained with a Japan Rigaku D/max-rA X-ray diffractometer with graphite monochromatized Cu Kα radiation ($\lambda = 1.5418$ Å). The samples were scanned at a scanning rate of 0.05°/s in the 2θ range of 10−70°.

Conventional and high-resolution electron microscopy (CTEM and HREM) examinations were performed with a Hitachi model H-800 with an attached EDAX (energy-dispersive X-ray fluorescence, EDAX 9100) system and a JEOL-2010 with an attached EDS (energy dispersive spectrum) system, both having an accelerating voltage of 200 kV.

X-ray photoelectron spectroscopy (XPS) were recorded on a VGESCALAB MKII X-ray photoelectron spectrometer, using nonmonochromatized Mg Kα X-ray as the excitation source, and choosing C 1s (284.60 eV) as the reference line.

Thermogravimetric analysis (TGA) and differential thermal analysis (DTA) traces were collected with a Shimadzu-50 thermoanalyzer apparatus under N_2 flow at 10 °C/min in the temperature range of 20−1000 °C.

Fourier transform infrared (FTIR) spectra were scanned using a Shimadzu IR-440 spectrometer in the region 4000−400 cm^{-1} at room temperature.

(12) Joint Committee on Powder Diffraction Standards (JCPDS). File number 7-415.

(13) Li, Y. D.; Ding, Y.; Qian, Y. T. *J. Phys., Chem. Solids* **1999**, *60* (1), 13.

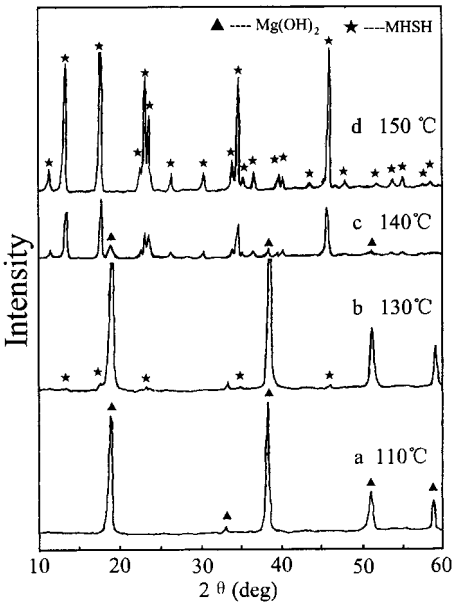

Figure 1. X-ray diffraction (XRD) patterns of the samples obtained at different temperatures: (a) 110 °C; (b) 130 °C; (c) 140 °C; and (d) 150 °C.

Results and Discussion

XRD and TEM Analysis. Phase identification of as-prepared sample was carried out using the XRD pattern shown in Figure 1d. All diffraction peaks can be indexed with respect to the orthorhombic structure $5Mg(OH)_2 \cdot MgSO_4 \cdot 3H_2O$, and the cell parameters calculated from these diffraction data are $a = 15.913$ Å, $b = 3.107$ Å, and $c = 13.371$ Å (RMS ERROR 4.36943E−05), which is in good agreement with the reported data.[12]

The structure and morphology of the sample were observed by TEM and HREM. Samples were prepared by placing a drop of dilute alcohol suspension of MHSH that was dispersed by ultrasonication onto carbon-coated copper grids and holey micromesh copper support, respectively, for observation in an electron microscope. The typical TEM image of the sample is illustrated in Figure 2f. The MHSH crystals display rodlike morphology with diameters ranging from 0.3 to 2 μm and lengths typically exceeding 40 μm. Electron diffraction (ED) patterns of the sample indicate that there exists an interesting superlattice structure which will be discussed in the following sections.

The temperature dependence of the reaction is investigated as summarized in Table 1. When the reaction temperature is below 110 °C, only $Mg(OH)_2$ can be obtained (see Figure 1a). The $Mg(OH)_2$ products mainly exhibit a hexagonal plate shape together with some needle-shaped morphology (see Figure 2a) which is characteristic of the hexagonal structure. When the temperature rises to 130 °C, a new phase appears although $Mg(OH)_2$ seems to remain the main phase. This new phase can be indexed as MHSH. A typical TEM image is shown in Figure 2b. The needle-shaped phase (area B) and a few whiskers (area A) coexist in sample 2. The ED pattern of the needle-shaped phase is shown in Figure 2c, which can be indexed to be $Mg(OH)_2$. Compared with the ED pattern of sample 1 (prepared at 110 °C, image not shown), some diffraction spots appear together with the diffraction rings which

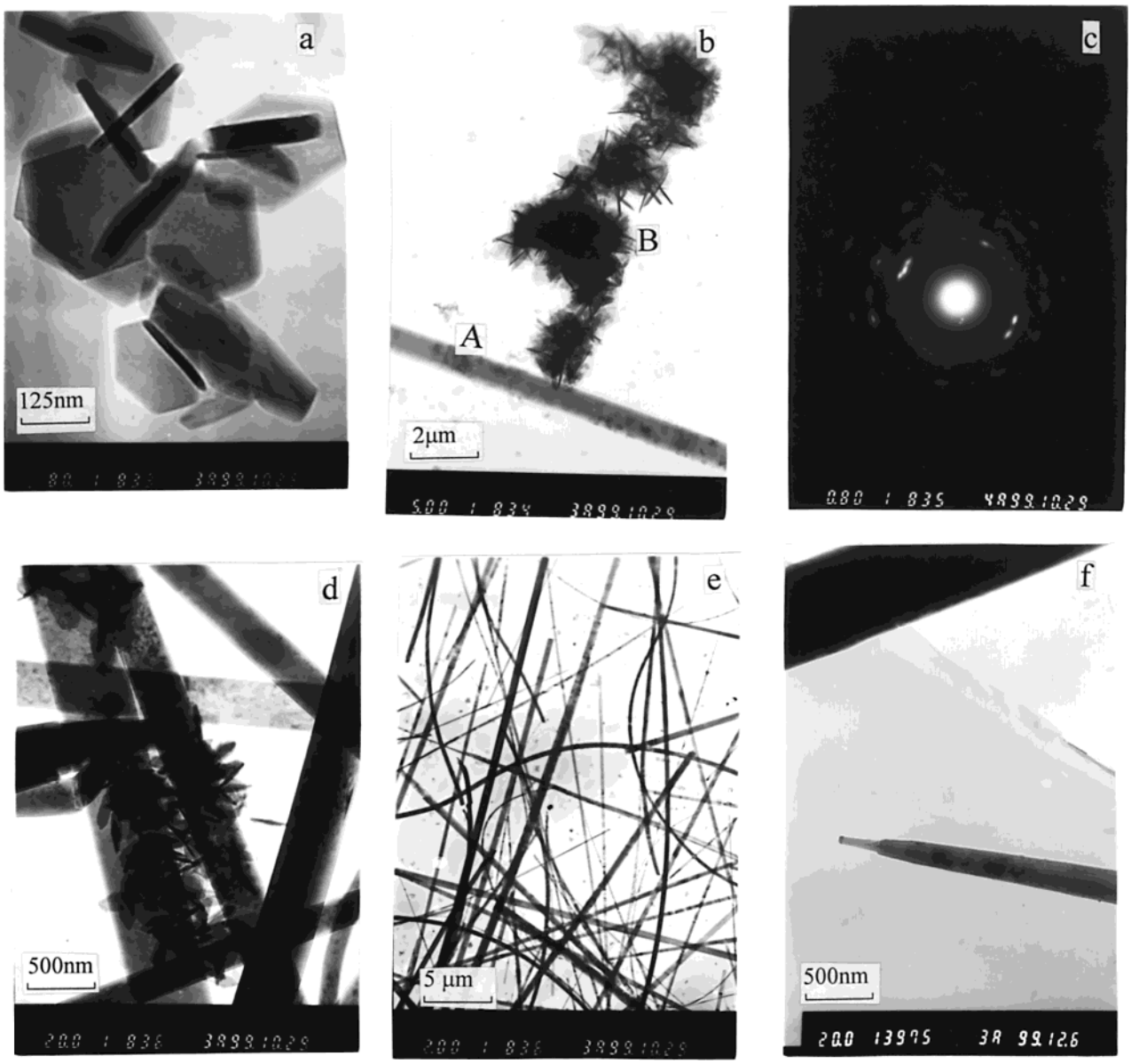

Figure 2. TEM images and diffraction patterns of the samples obtained at different temperatures: (a) 110 °C; (b), (c) 130 °C; (d), (e) 140 °C; and (f) 150 °C

Table 1. Temperature Dependence of the Reaction Synthesized from $MgSO_4$ and $NH_3 \cdot H_2O$ under Hydrothermal Conditions[a]

sample	*T* (°C)	phases (identified by XRD)
1	110	$Mg(OH)_2$
2	130	$Mg(OH)_2$* + MHSH
3	140	$Mg(OH)_2$ + MHSH*
4	150	MHSH

[a] Phases marked with an asterisk (*) represent the main phase.

means better crystallinity of the $Mg(OH)_2$. EDAX analysis of sample 2 indicates that the area A consists of Mg and S, while in area B, only Mg is detected, which further approves that the whiskers contain MHSH and the needle phase is $Mg(OH)_2$. Oxygen and hydrogen are not detected because the EDAX attached in H-800 can only determine elements after sodium. Sample 3 is prepared at 140 °C. Most of the $Mg(OH)_2$ is found to have transformed into the MHSH phase (see Figure 1c) which is also supported by the TEM analysis (see Figure 2d,e). From Figure 2e, almost all of the MHSH products possess a straight, fibrous structure with a size of (0.3−2) × (40−100) μm. When the temperature reaches 150 °C, pure MHSH can be obtained, which can be identified either by XRD (Figure 1d) or by TEM (see Figure 2f). Higher temperatures above 150 °C will generate better crystallinity but larger crystallite size of the whiskers. From the results mentioned above, the transformation from $Mg(OH)_2$ to MHSH starts at about 120 °C, and the MHSH phase replaces the $Mg(OH)_2$ phase as the main phase at about 135 °C. These results are consistent with the data described in other literature.[4,5,8]

HREM and SAED Observations. High-resolution electron microscopy (HREM) is a powerful method for structure analysis in the atomic scale, and thus might provide further insight into the structure of an individual MHSH whisker. Figure 3a illustrates a low-magnification HREM image of as-prepared sample. The "two" whiskers shown in the image are actually branches of a single crystallite. The corresponding ED pattern along the [110] zone axis direction is shown in Figure 3b (for area A in Figure 3a), where an interesting superlattice is observed. The additional diffraction spots

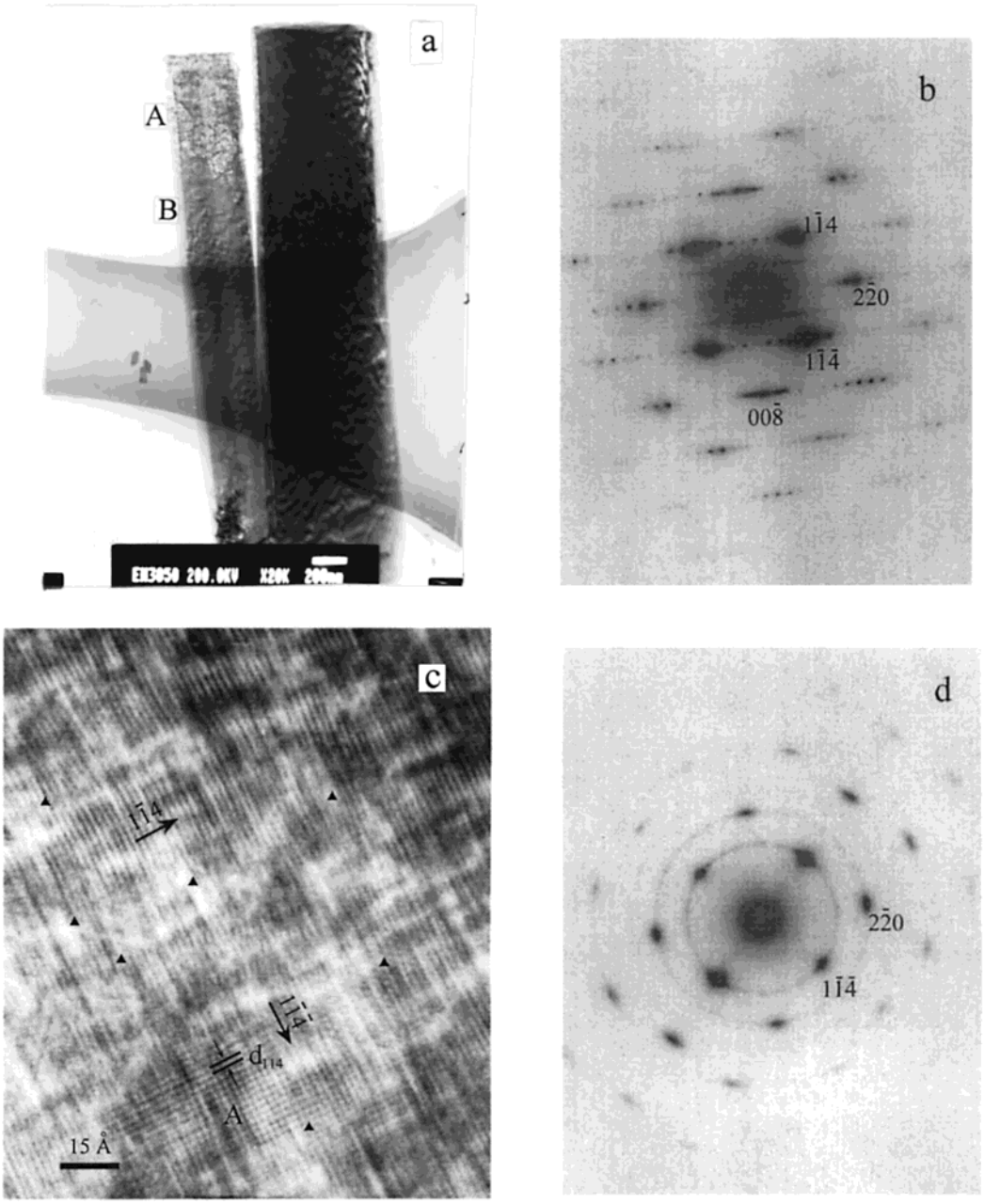

Figure 3. HREM images and SAED patterns of the sample obtained at 150 °C low-magnification HREM image; ED pattern before the radiation of high-energy electron beam, taken along the [110] zone orientation; high-magnification HREM image; ED pattern after the radiation of high-energy electron beam.

along the 1$\bar{1}$0 direction indicate the presence of a presently unknown 8 times superlattice. This "large" structure should be clearly observed in the HREM, but unfortunately, when an electron beam (EB) of elevated intensity is focused on the sample, and the superlattice quickly disappears. Figure 3c shows a typical image of the sample after this transformation. Despite the disappearance of the superstructure, most of the preferential [1$\bar{1}$4] orientation is preserved. In area A, a microcrystallite (zone [110]) shows a quasi-square two-dimensional fringe. This is because the (1$\bar{1}$4) plane and the (1$\bar{1}\bar{4}$) plane meet at an angle of about 84.7°. The observed interspacing of $d_{(114)}$ is about 2.2 Å which is consistent with the ideal value of 2.253 Å. Besides, it should be noted that the sample consists of many domains with a size of 2 × 3 nm (marked by arrows). Although it cannot be concluded whether these domains are existed before or after the radiation of the EB, we believe that these domains and the metastable superlattice may have potential value to both scientific research and application. Figure 3d demonstrates the ED pattern at the same area after the radiation of elevated-energy EB. One can see the diffraction spots for superstructure disappear with the appearance of a series of diffraction rings, while the basic diffraction spots still exist as in Figure 3b. These diffraction rings may result from the partial polycrystallizing of the sample upon interaction with the EB. These changes can also be clearly seen in Figure 3a. The color of area

(14) Wagner, C. D.; Riggs, W. M.; Davis, L. E.; Moulder, J. F.; Muilenberg, G. E. *Handbook of X-ray Photoelectron Spectroscopy*; Perkin-Elmer, Physical Electronics Division: Norwalk, CT, 1979.

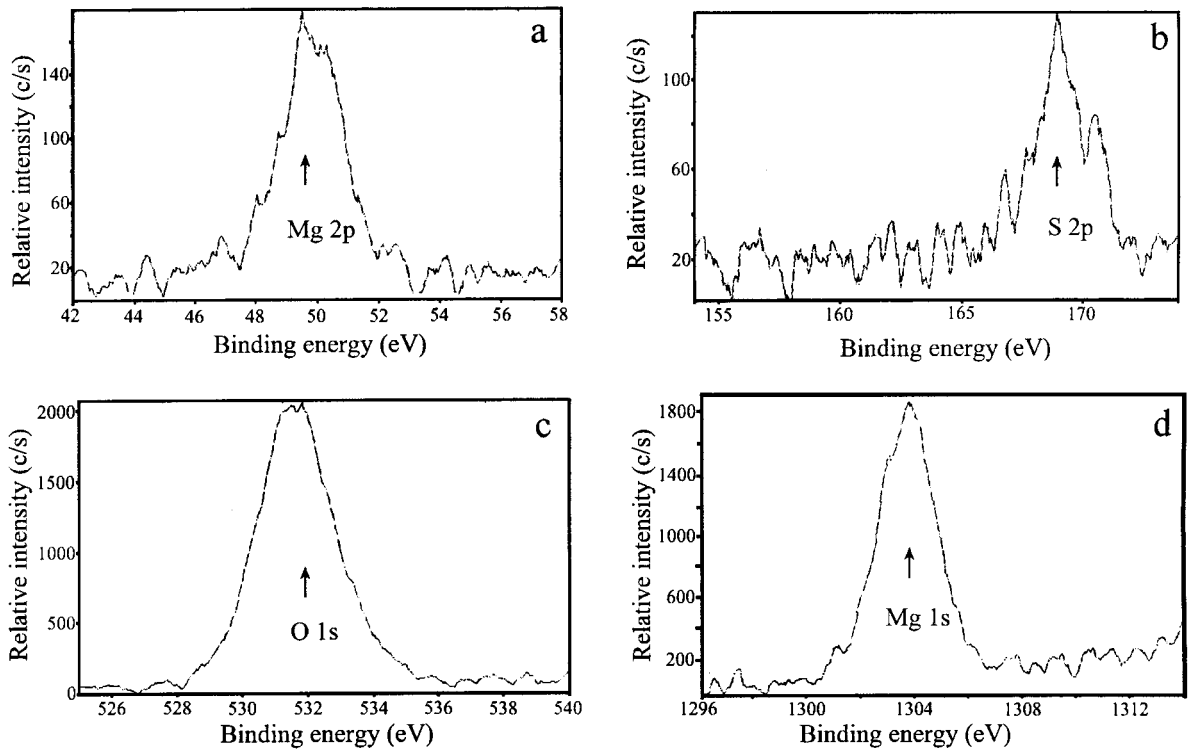

Figure 4. XPS spectra of the MHSH sample; close-up surveys for (a) Mg 2p core, (b) S 2p core, (c) O 1s core, and (d) Mg 1s core.

A which has undergone the radiation of EB is less dark than that of area B which has not. The chemical microanalysis by EDS from local area gives a typical composition of Mg:S:O in 5.34:1:14.8 atomic ratio. The concentration ratio of Mg to S in the sample is less than the reported magnitude (Mg:S = 6:1), which might be related to a specific defect structure of the superlattice.

Chemical Composition Analysis. X-ray photoelectron spectra (XPS) were measured to derive composition information about the MHSH samples. Figure 4a−d depicts high-resolution XPS spectra taken for the Mg, S, and O regions of the sample. The peak at about 49.50 eV is attributed to Mg (2p) (see Figure 4a) which is very close to the data for Mg (2p) in $Mg(OH)_2$ (49.50 eV).[14] The peak at 168.90 eV corresponds to S (2p) binding energy (see Figure 4b) while the peak at about 531.90 eV can be attributed to O (1s) (see Figure 4c).[14] The peak broadening in Mg (2p) and O (1s) spectra indicates that both of them have more than one environment. Figure 4d describes the spectrum of Mg (1s).

Peak areas of the Mg (2p), S (2p), and O (1s) cores were measured and used to calculate the chemical composition of the sample. Areas were determined by fitting each of the curves using a nonlinear least-squares curve-fitting program,[15] and taking the area of the fit peak. Because the shape of the background was uncertain, the absolute areas are accurate to an error of about 12%. However, the background is kept the same for all fits, and so the relative error is much smaller. An empirical correction was made for the pass energy variation between two scans when there was a difference. The quantification of the peaks gives the ratio of Mg:S:O of 5.28:1:14.35 which is close to the results obtained by EDS analysis in HREM.

Table 2. Chemical Composition of MHSH

element (wt %)	calculated composition for theoretical MHSH phase				experimental results
	5−1−3	5−1−2	4.34−1−3	4.34−1−2	
Mg	31.30	32.56	30.37	31.70	31.58[b]
S	6.87	7.15	7.49	7.82	7.79[b]
O	58.39	57.17	58.71	57.38	57.63[b]
H	3.43	3.13	3.44	3.10	3.0[a]

[a] Obtained by elemental analysis. [b] Calculated from EDS results: Mg:S:O = 5.34:1:14.8 using H 3.0 wt % as a reference.

Since elemental hydrogen (H) is undetectable either by XPS analysis or by EDS scan, elemental analysis (EA, for C,H,N) was preformed with a Perkin-Elmer (PE-240C) spectrometer to determine the component of hydrogen in the sample. This gave the result of 3.0 (wt %) for H. The amount of carbon and nitrogen is under the experimental error, and thus cannot be thought to be existent in the sample. Analysis of the results given by EDS and EA measurements can give a composition of 31.58 wt % Mg, 7.79 wt % S, 57.63 wt % O, and 3.0 wt % H, corresponding to a nearest stoichiometry $4.34Mg(OH)_2{\cdot}MgSO_4{\cdot}2H_2O$ (see Table 2) which is thought to be derived from $5Mg(OH)_2{\cdot}MgSO_4{\cdot}2H_2O$ phase. Here, the XPS data is only referred to because the XPS technique detects the information from the surface area of the sample while the EDS scan is a more direct method. As compared to the well-known 5−1−3 phase, we think that the amount of crystallized water (H_2O) is 2 which is in agreement with the results reported by Miyata.[16] One possible explanation for one more H_2O in other literature[1−12] is that their samples were not dry enough. It should be pointed out that possible experimental error might change the results of composition, especially for the slight molecular change of one

(15) Peakfit version 3.10, Jandel Scientific: San Rafael, CA, 1992.

(16) Miyata, S.; Okada, A.; Hirose, T. *Eur. Pat. Appl. EP* **1985**, *132*, 610 (Cl. C01F5/06).

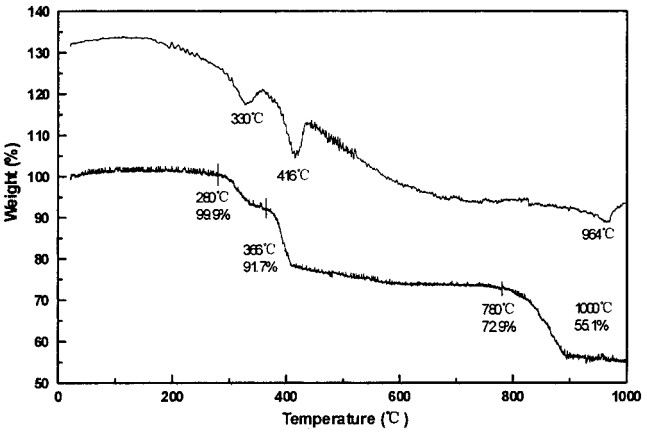

Figure 5. TGA-DTA trace of the sample heated in N_2 flow from 20 to 1000 °C

H_2O. However, the information from the thermal analysis also proves that the amount of the crystallized water in the sample is more likely to be 2 which will be discussed in detail in the next section. It should be noted that the value of Mg lack is about 0.66, which means the ratio of Mg occupancy of the ideal MHSH structure is about 0.89 (5.34/6) or 0.868 (4.34/5), which is very close to 0.875 ($^7/_8$). Thus, the Mg lack in structure is probably the origin of the 8-time superlattice. It is admitted that the precise structure determination should finally be dependent upon the X-ray structure refinement by the Patterson method, and these works are currently underway.

TGA and DTA Analyses. TGA-DTA technique and corresponding XRD phase characterization were used to analyze the thermal behavior of the MHSH sample. One can see from Figure 5, three main weight loss steps are found on the TGA curve and corresponding endothermic peaks are observed near 330, 416, and 964 °C. In the temperature range of 20−280 °C, no weight loss is observed, and the corresponding in situ XRD patterns also show no differences with that for the sample at room temperature. Litvinov[11] and Kahle[4] even reported that the structure of $5Mg(OH)_2{\cdot}MgSO_4{\cdot}3H_2O$ was stable with heating to <280 °C, but one molecular of water loss would occur in the temperature range of 20−175 °C. Thus, we think the additional water in their sample is more probably to be the physically combined water, and the 5−1−3 phase might actually be the 5−1−2 phase.

In the temperature range from 280 to 366 °C, an 8.2 wt % weight loss can be attributed to the loss of two hydrational waters by the reaction:

$$4.34Mg(OH)_2{\cdot}MgSO_4{\cdot}2H_2O \xrightarrow{-2H_2O} 4.34Mg(OH)_2{\cdot}MgSO_4 \quad (1)$$

The weight loss calculated from the above-mentioned equation is 8.8%. This is also substantiated by the corresponding XRD patterns which show the basic crystal structure of the sample is maintained in this temperature range.

The following weight loss of about 18.8 wt % between 366 and 780 °C was ascribed to the decomposition of brucite:

$$4.34Mg(OH)_2{\cdot}MgSO_4 \xrightarrow{-4.34H_2O} 4.34MgO + MgSO_4 \text{ (19.1 wt \%, loss calculated)} \quad (2)$$

Let it be supposed that the structure do be the 5−1−3 phase, and a third molecular of water loss in this temperature range, a total amount of 5.34 water loss would occur, and a 22.5 wt % weight loss should be seen according to the following equations:

$$4.34Mg(OH)_2{\cdot}MgSO_4{\cdot}3H_2O \xrightarrow{-2H_2O} 4.34Mg(OH)_2{\cdot}MgSO_4{\cdot}H_2O \text{ (8.4 wt \%)} \quad (3)$$

$$4.34Mg(OH)_2{\cdot}MgSO_4{\cdot}H_2O \xrightarrow{-5.34H_2O} 4.34MgO + MgSO_4 \text{ (22.5 wt \%)} \quad (4)$$

However, only a loss of 18.8 wt % was detected, which further substantiates that the sample is a 5−1−2 or 4.34−1−2 phase.

The XRD patterns in this temperature range are rather complex. The peaks of MHSH phase decrease in intensity, and a series of other diffraction peaks appear which are difficult to be completely indexed. This might result from the structure decomposition of the initial MHSH phase and the appearance of some intermediate phase. However, the appearance and increase of the magnesium oxide (MgO) phase is of no question because the new peaks at 2θ 43.0° and 62.2° are characteristic peaks of periclase's (200) and (220) planes according to the XRD analyses.

The final pronounced weight loss of 17.8 wt % between 780 °C and 1000 °C is assigned to the decomposition of $MgSO_4$ into MgO:

$$MgSO_4 \xrightarrow{-SO_3} MgO \quad (5)$$

In terms of the decomposition reaction, a weight loss of 19.5 wt % should be achieved. We owe it to the incompleteness of the decomposition reaction. This is consistent with the FTIR spectral study, which will be discussed in the next section. The XRD pattern of the sample calcined at 950 °C indicated that *pure* MgO was obtained. The $MgSO_4$ is undetected in the XRD analysis because of its relatively low quantity in the sample as compared to MgO.

FTIR Characterization. Fourier transform infrared (FTIR) spectra were also used to investigate the thermal behavior of the MHSH sample. Samples were calcined in different temperatures and then mulled in KBr wafers. Figure 6a illustrates the FTIR spectrum of the MHSH sample as prepared. A sharp absorption band is found at about 3680 cm^{-1} which is the characteristic frequency of the hydroxyl group (OH) stretching vibration.[17,18] As the temperature rises up from room temperature to 380 °C, and until finally to 950 °C, this OH absorption band gradually diminishes in intensity and disappears (see Figure 6b−e). The strong sharp band near 3420 cm^{-1} and the medium band near 1633 cm^{-1}

(17) Nyquist, R. A.; Kagel, R. O. *Infrared spectra of inorganic compounds*; Academic Press: New York, 1971.
(18) Wang, J. A.; Novaro, O.; Bokhimi, X.; López, T.; Gómez, R.; Navarrete, J.; Llanos, M. E.; López-Salinas, E. *Mater. Lett.* **1998**, 35, 317.

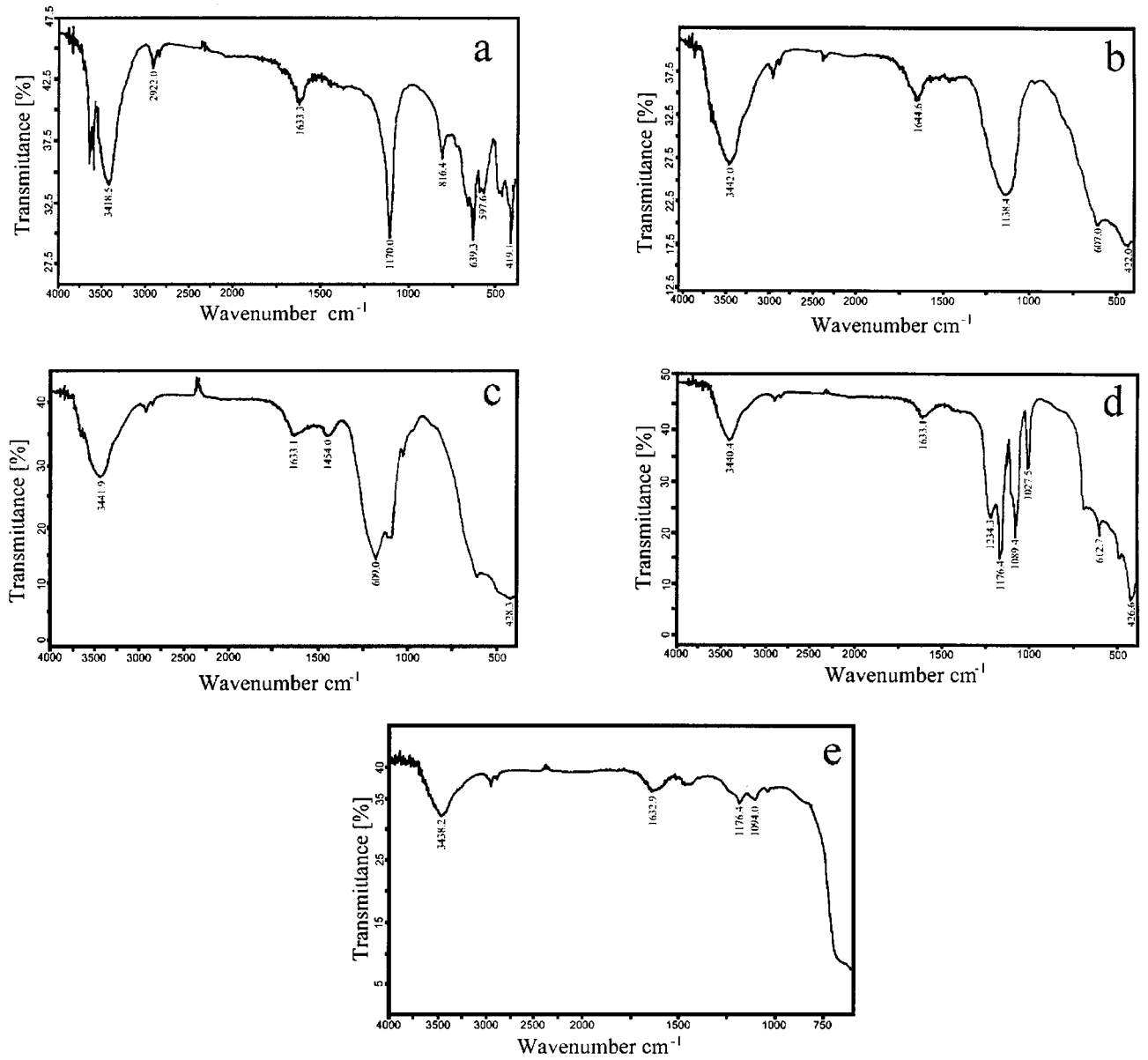

Figure 6. FTIR spectra of the sample calcined at different temperature: (a) without calcination, (b) 380 °C, (c) 600 °C, (d) 840 °C, and (e) 950 °C.

can be assigned to the OH stretching vibration and H−O−H bending motion, respectively, for the water of hydration.[17] The amount of absorbed water or free water, if present, is quite small since free water has a strong broad absorption band centered in the region 3200−3400 cm^{-1} and a H−O−H bending mode near 1650 cm^{-1}. The sharp band at 1117 cm^{-1} and the multiple bands from 570 to 680 cm^{-1} are characteristic absorption bands for SO_4^{2-}. The absorption bands above the 3700 cm^{-1}, below the 500 cm^{-1} and the peak at 816.4 cm^{-1} are not easily to index. Since they tend to diminish in relative intensity as the treatment temperature increases (see Figure 6b−e), we think that they might result from the internal modes involving vibrations of the crystal structure or lattice. For samples calcined at 380, 600, and 840 °C (see Figure 6b−d), the relative intensity of OH^{-1} absorption bands declines gradually and the bands related to the crystal structure disappear. One can note that the bands for SO_4^{2-} (1000−1240 cm^{-1}) occur when the treatment temperature is raised to 840 °C (see Figure 6d). Actually, this is also in agreement with the fact because when the sample is calcined at 840 °C, it is mainly comprised of MgO and $MgSO_4$. Since MgO has no obvious absorption band in the region 800−4000 cm^{-1}, only the absorption band of $MgSO_4$ can be detected. In other words, the detected resolution of $MgSO_4$ has been magnified. When the treatment temperature reaches 950 °C (see Figure 6e), a steep decline of the absorption bands for SO_4^{2-} occurs, indicative of the decomposition of $MgSO_4$ into MgO. In the meantime, a clear indication of the magnesium oxide phase can be noted. This is supported by the diagnostic parabola-like graph, which is almost perfectly symmetrical to the axis of 500 cm^{-1} .[17] Although the full spectra, especially in the far-infrared region between 400 and 200 cm^{-1}, is not attainable owing to the limitation of the instrument, its left branch is still enough to determine that MgO is the major product. Weak absorption bands are also observed for $MgSO_4$ due to the incompleteness of the decomposition reaction. These results are generally in agreement with the TGA results and the corresponding XRD analyses. There still

seems to be weak bands at 3438 and 1632 cm^{-1}, indicating H_2O. This is because the FTIR spectral measurement is carried out in air and the absorption of water on the surface of the sample is always unavoidable. A band near 2922 cm^{-1} exists in the whole measured temperature range of 20−950 °C which is associated with a saturated C−H vibration from some impurity in the KBr crystals.

Conclusions

In summary, magnesium hydroxide sulfate hydrate whiskers with an aspect ratio larger than 100 have been prepared by a hydrothermal method using $MgSO_4$ and $NH_3 \cdot H_2O$ as the starting reactants. In comparison to some other works,[4−6] where $MgSO_4$ and $Mg(OH)_2$ (or MgO) were used as the starting reactants, this method is simple and controllable, and thus, the produced MHSH can be of high purity. Structural features, chemical composition, and thermal behavior of the product have been systematically investigated using various techniques. The product is found to possess a composition of $4.34Mg(OH)_2 \cdot MgSO_4 \cdot 2H_2O$ with an interesting superlattice structure. This superstructure is metastable under the radiation of a high-energy electron beam. The sample will lose two hydration waters near 330 °C, decompose at a higher calcination temperature, and eventually transform into MgO at about 1000 °C. With its unusual structure, this material may be potentially useful for further scientific research and application studies.

Acknowledgment. We are indebted to Professor Zhou Guien and Ji Mingrong for assistance with the XRD and XPS analyses, to Dr. Wang Liangbin and Professor Li Qianrong for obtaining the TGA-DTA and EA results, and to Dr. Yang Li and Liu Xianming for help with the TEM analysis. We also would like to express our gratitude to Ms. Chen Kunsong for her generous help with the IR experiment and Dr. Lu Jun, Sun Yugang, Wu Hao, and Zhang Guohui for their valuable comments and assistance with this study. This work is supported by the National Natural Science Foundation of China and the National Nanometer Materials Climbing Project.

CM000249F